Recent Heavy Ion Results from the ATLAS Experiment

Mariusz Przybycień

AGH University of Science and Technology, Cracow, Poland

(on behalf of the ATLAS Collaboration)

Devoted to the 90th anniversary of Academician A.M. Baldin

XXIII International Baldin Seminar on High Energy Physics Problems

Relativistic Nuclear Physics & Quantum Chromodynamics

September 19 - 24, 2016, Dubna, Russia

Recent heavy ion results from Pb+Pb and p+Pb

Electroweak bosons and Quarkonium:

- Measurement of the production and lepton charge asymmetry of W bosons in PbPb collisions at $\sqrt{s_{\mathrm{NN}}} = 2.76$ TeV with the ATLAS detector. Eur. Phys. J. C (2015) 75:23
- Z boson production in p+Pb collisions at $\sqrt{s_{\mathrm{NN}}} = 5.02$ TeV measured with the ATLAS detector. Phys. Rev. C 92 (2015) 044915
- Measurement of $W \to \mu\nu$ production in p+Pb collision at $\sqrt{s_{\mathrm{NN}}} = 5.02$ TeV with the ATLAS detector at the LHC. ATLAS-CONF-2015-056
- Centrality, rapidity and transverse momentum dependence of isolated prompt photon production in lead-lead collisions at $\sqrt{s_{\mathrm{NN}}}$ =2.76 TeV measured with the ATLAS detector. Phys. Rev. C 93 (2016) 034914
- Study of J/Ψ and $\Psi(2S)$ production in $\sqrt{s_{\mathrm{NN}}} = 5.02$ TeV p+Pb and $\sqrt{s} = 2.76$ TeV pp collisions with the ATLAS detector. ATLAS-CONF-2015-023

Production of jets in Pb+Pb collisions:

- Measurements of the nuclear modification factor for jets in Pb+Pb collisions at $\sqrt{s_{\mathrm{NN}}}$ =2.76 TeV with the ATLAS detector. Phys. Rev. Lett. 114, 072302 (2015)
- Properties of dijet asymmetries measured with 2.76 TeV/nucleon Pb+Pb collisions in ATLAS at the LHC. ATLAS-CONF-2015-052
- Internal structure of jets measured in Pb+Pb and pp collisions with the ATLAS detector at the LHC. ATLAS-CONF-2015-055

Recent heavy ion results from Pb+Pb and p+Pb

- Measurement of the production of neighbouring jets in lead-lead collisions at $\sqrt{s_{\mathrm{NN}}}$ =2.76 TeV with the ATLAS detector. Phys. Lett. B751 (2015) 376
- Transverse momentum, rapidity, and centrality dependence of inclusive charged-particle production in $\sqrt{s_{\mathrm{NN}}}$ =5.02 TeV p+Pb collisions measured by the ATLAS experiment. arXiv:1605.06436, $\rightarrow$ PLB

Bulk particle collectivity:

- Measurement of FB multiplicity correlations in Pb+Pb, p+Pb and pp collisions with the ATLAS detector. arXiv:1606.08170, $\rightarrow$ PRC
- Femtoscopy with identified charged pions in proton-lead collisions at $\sqrt{s_{\mathrm{NN}}} = 5.02$ TeV with ATLAS. ATLAS-CONF-2016-027
- Measurements of long-range azimuthal anisotropies and associated Fourier coefficients in pp collisions at 5.02 and 13 TeV and p+Pb collisions at 5.02 TeV with the ATLAS detector. ATLAS-CONF-2016-026
- Measurement of the correlation between flow harmonics of different order in lead-lead collisions at $\sqrt{s_{\mathrm{NN}}} = 2.76$ TeV with the ATLAS detector. Phys. Rev. C 92 (2015) 034903

Ultra-peripheral Pb+Pb collisions (UPC):

- Measurement of high-mass dimuon pairs in ultra-peripheral lead-lead collisions at $\sqrt{s_{\mathrm{NN}}}$ =5.02 TeV with the ATLAS detector at the LHC. ATLAS-CONF-2016-025

Probing Quark-Gluon Plasma

Collisions of heavy ions (HI) enable to investigate QCD in the limit of high densities and temperatures reached in deconfined medium - the Quark Gluon Plasma (QGP).

- We can study properties of QGP by:
  - using hard probes of different scales: electroweak bosons, jets, heavy quarks, ...

    Assume factorisation: hard probes are produced early in the HI collision, in a process which cross section is not changed by presence of strongly interacting medium, i.e. can by calculated in pQCD. Passing through the medium hard probes interact weakly or strongly with it providing information on its properties.

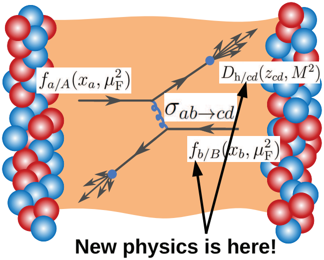

  - measuring parameters describing collective behaviour of the medium.

- Heavy ions are intense sources of photons: in ultra-peripheral collisions one can study two photon interactions, diffraction, ...

Yields of hard processes in HI collisions are expected to scale with the number of binary nucleon-nucleon collisions, N_{coll}, which depends on the centrality of the collision.

Central collisions: large overlap of nuclei $\Rightarrow$ high N_{coll} and high number of nucleons participating in the collision, N_{part}.

Peripheral collisions: small overlap of nuclei $\Rightarrow$ small N_{coll} and small N_{part}.

The ATLAS detector

Detector coverage:

Inner Detector (ID):
$|\eta| < 2.5$

Calorimeter (CAL):
$|\eta| < 3.2$ (EM)
$|\eta| < 4.9$ (HAD)
$3.2 < |\eta| < 4.9$ (FCal)

Muon Spectrometer (MS):
$|\eta| < 2.7$

Zero Degree Cal. (ZDC):
$|\eta| > 8.3 \quad @z = \pm 140$ m

MB Trig. Scint. (MBTS):
$2.1 < |\eta| < 3.9$

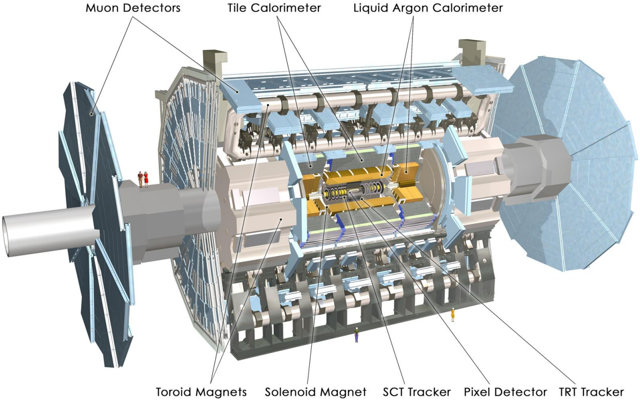

Magnetic fields:

- 2T solenoid field in ID
- Toroidal field in MS

Identification of minimum-bias Pb+Pb collisions:

measurement of spectator neutrons in Zero Degree Calorimeters (ZDC) and charged particles (pulse hight and arrival times) in Minimum Bias Trigger Scintillators (MBTS).

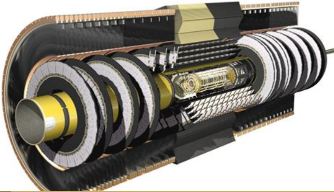

Pb+Pb data (2010, 2011, 2015): $\sqrt{s_{\mathrm{NN}}} = 2.76$ TeV.
p+Pb data (2012, 2013): $\sqrt{s_{\mathrm{NN}}} = 5.02$ TeV.

Centrality determination in Pb+Pb and p+Pb

- Centrality is measured using forward calorimeters ($3.2 < |\eta| < 4.9$):

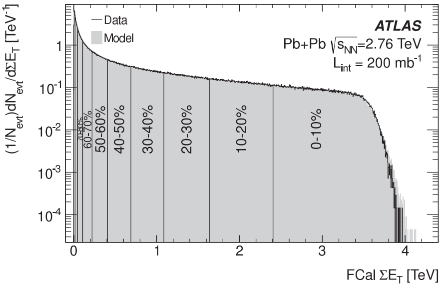

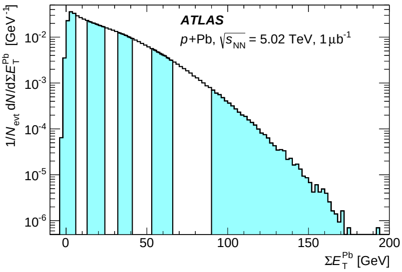

- in Pb+Pb use sum of E_T on both sides,
- in p+Pb use sum of E_T on Pb-going side only,
- for Pb+Pb use Glauber MC for geometry,
- for p+Pb use both Glauber and Glauber-Gribov color fluctuation model (PLB 633: 245 (2006)).
- Average number of participants (N_{part}) for each centrality bin resulting from fits to the measured E_T distribution for p+Pb.

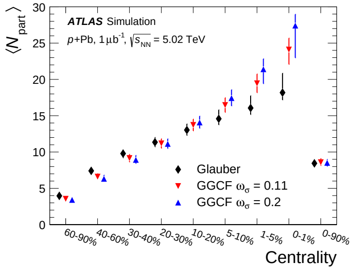

Electroweak bosons and quarkonium

Electroweak bosons in heavy ion collisions

- Electroweak (EW) bosons and their leptonic decay products do not interact strongly. Therefore if formed in a hard parton-parton interaction at a very early stage of the Pb+Pb or p+Pb collision they carry out unmodified information about the geometry of the nuclei at the collision time.

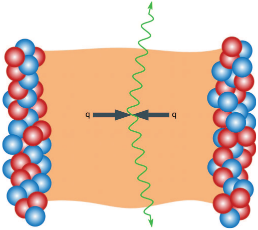

- In LO, W^+ (W^-) bosons are produced by interactions of u (d) valence quarks and $\bar{d}$ ($\bar{u}$) sea quarks.
  Information about nPDF modification can be obtained from lepton charge asymmetry.

- Z and W boson production yields per binary collision do not depend on centrality.
  This is consistent with a view of heavy ion collisions as a superposition of nucleon-nucleon collisions.

Phys. Rev. Lett. 110, 022301 (2013)

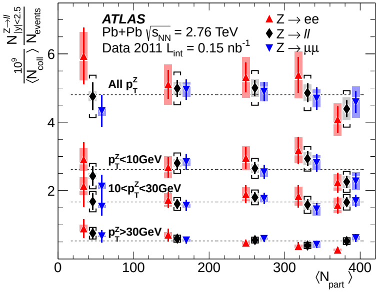

Eur. Phys. J. C75 (2015) 23

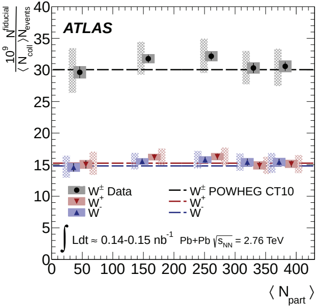

W boson production in Pb+Pb collisions

- nPDF modifications are explored with differential $W \to \ell\nu_\ell$ production yields per binary nucleon-nucleon collision and the lepton charge asymmetry, as a function of $|\eta_\ell|$.
- Lepton charge asymmetry: $A_\ell(\eta_\ell) = \frac{\mathrm{d}N_{W^+\to\ell^+\nu_\ell}/\mathrm{d}\eta_\ell - \mathrm{d}N_{W^-\to\ell^-\bar{\nu}_\ell}/\mathrm{d}\eta_\ell}{\mathrm{d}N_{W^+\to\ell^+\nu_\ell}/\mathrm{d}\eta_\ell + \mathrm{d}N_{W^-\to\ell^-\bar{\nu}_\ell}/\mathrm{d}\eta_\ell}$
- Data are well described by the superposition of nucleon-nucleon collisions.
- Data can not distinguish between nucleon PDF and that incorporating nuclear effects.
- The asymmetry in Pb+Pb collisions differ significantly from that in pp collisions because of significant number of nuetrons in lead nuclei, ${}^{208}_{82}$Pb.

Eur. Phys. J. C75 (2015) 23

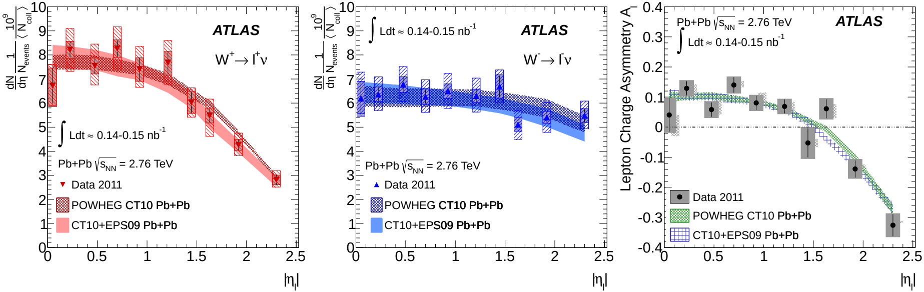

Electroweak bosons in p+Pb collisions

- p+Pb are used to differentiate between initial and final state effects in HI collisions.
- ATLAS data: $\sqrt{s_{\mathrm{NN}}} = 5.02$ TeV (nucleon en. in Pb: 1.57 TeV), $\mathcal{L}_{pA} = 28.1$ nb^{-1}
- Due to asymmetric collision CM is shifted in rapidity towards proton direction by 0.465 units: $y^{\star} = y^{\mathrm{lab}} - 0.465$
- Total cross sections in function of $y^{\star}_{Z}$ and $\eta^{\mu}_{\mathrm{lab}}$ have been measured for Z and $W^{\pm}$.

- Small excess for Z and W^{-} in Pb-going direction is observed in data.
- nPDF scenario is sligthly prefered by Z data.

Phys. Rev. C 92, 044915 (2015)

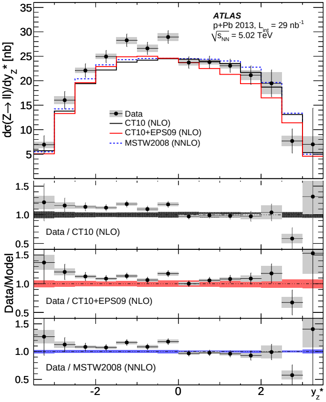

ATLAS-CONF-2015-056

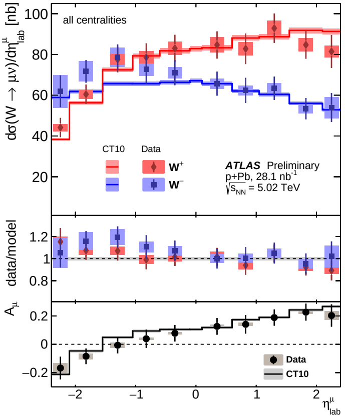

Electroweak bosons in p+Pb collisions

- Differential yields per event scaled by $\langle N_{\rm coll}\rangle$ for Z and $W^{\pm}$ bosons are shown as a functions of $y^{\star}_{Z}$ or $\eta^{\mu}_{\rm lab}$, in three centrality classes.
- Differences between data and models are larger in central than in peripheral collisions (Z boson yields).
- Possible centrality dependece of nuclear modifications in W bosons yields?

Phys. Rev. C 92, 044915 (2015)

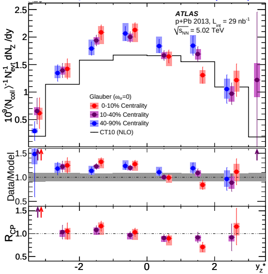

ATLAS-CONF-2015-056

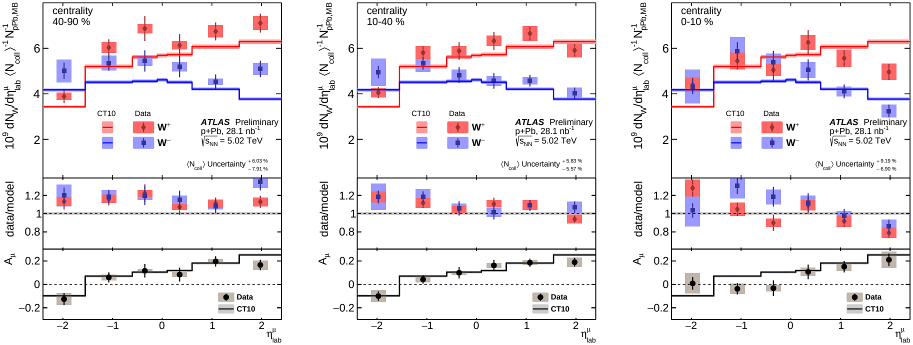

Isolated prompt photon production in Pb+Pb

- Sources of prompt photons: quark-gluon Compton scattering $qg \rightarrow q\gamma$ and production of hard photons during parton fragmentation $\bar{q}q \rightarrow g\gamma$.
- Prompt photons being colorless are transparent to the subsequent evolution of the QGP and probe the very initial stages of collision i.e. nuclear modifications to PDF.

- Ratios of scaled yields of prompt photons to the JETPHOX pp predictions are shown in function of photon p_{T}, in different centrality classes and in central and forward rapidity regions.
- At current precision of data nuclear modification to PDF seems not to be necessary.
- Cancelation of many systematic uncertainties in the ratio: forward to central.

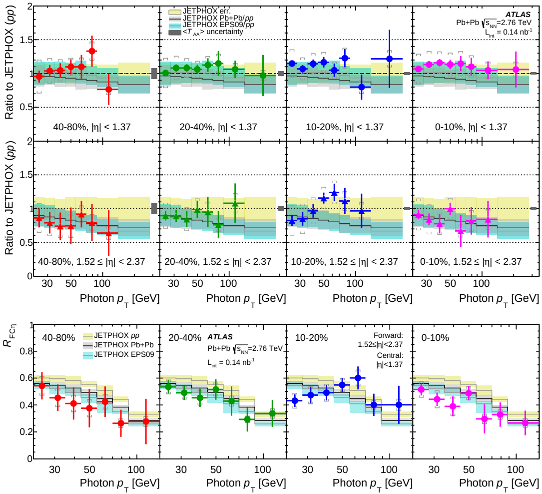

Phys. Rev. C 93, 034913 (2016)

Quarkonium production in p+Pb collisions

- Quarkonium states of J/ψ and $\psi(2S)$ as well as $\Upsilon(nS)$ have been measured in p+Pb collisions at $\sqrt{s_{\rm NN}}$ =5.02 TeV and in pp collisions at $\sqrt{s} = 2.76$ TeV, using $\mu^+\mu^-$ decay channels.
- Maximum likelihood fit to $m_{\mu\mu}$ and to *di-muon pseudo proper lifetime* $\tau = L_{xy}\frac{m_{\mu\mu}}{p_T}$ to extract signal yields and fraction from b-hadron decays.
- J/ψ and $\psi(2S)$ states have been recostructed in the range $8.5 < p_{\rm T}^{\mu\mu} < 30$ GeV and $-1.5 < y^{\star}_{\mu\mu} < 1.5$.
- $\Upsilon(nS)$ states have been extracted from the fit to $m_{\mu\mu}$ in the range $p_{\rm T}^{\mu\mu} < 40$ GeV and $-2.25 < y^{\star}_{\mu\mu} < 1.2$.

ATLAS-CONF-2015-050

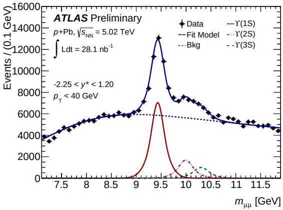

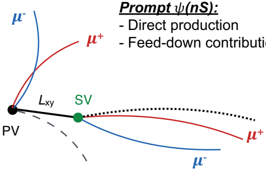

ATLAS-CONF-2015-023 →

Prompt ψ(nS):
- Direct production
- Feed-down contribution

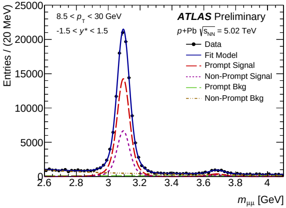

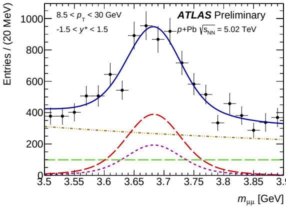

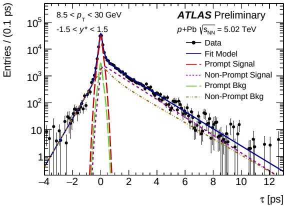

Nuclear modification factor

- Nuclear modification factor ($A^{\mathrm{Pb}} = 208$):

$$R_{p\mathrm{Pb}} = \frac{1}{A^{\mathrm{Pb}}} \frac{\mathrm{d}^2\sigma_{\psi}^{p+\mathrm{Pb}}/\mathrm{d}y^{\star}\mathrm{d}p_{\mathrm{T}}}{\mathrm{d}^2\sigma_{\psi}^{pp}/\mathrm{d}y\mathrm{d}p_{\mathrm{T}}}$$

- pp reference is constructed using interpolations.
- For J/ψ and $\psi(2S)$, the $R_{p\mathrm{Pb}}$ is above unity and does not show any significant trend in p_{T} or $y^{\star}$.

ATLAS-CONF-2015-023 →

- Upsilon $R_{p\mathrm{Pb}}$ show similar p_{T} and $y^{\star}$ dependence as charmonium states.

ATLAS-CONF-2015-050

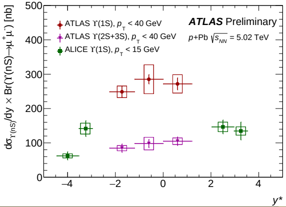

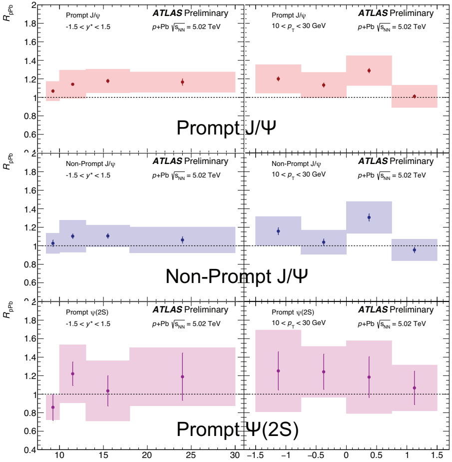

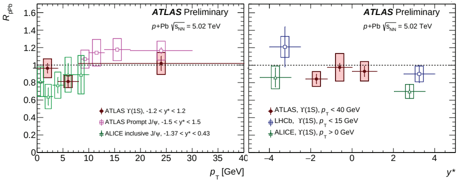

Production of jets

Inclusive jet suppression

- High transverse momentum partons, produced in hard scattering process, propagating through the medium of strongly interacting nuclear matter, lose energy, resulting in the phenomenon of 'jet quenching'.
- Magnitude of suppresion is expected to depend on both the p_{T} dpendence of energy loss as well as the shape of initial jet p_{T} spectrum.
- Suppression is quantified by the nuclear modification factor:

$$R_{AA} = \frac{1}{N_{\mathrm{evt}}} \frac{1}{\langle T_{AA} \rangle} \left(\left. \frac{\mathrm{d}^2 N_{\mathrm{jet}}}{\mathrm{d}p_{\mathrm{T}}\mathrm{d}y} \right|_{\mathrm{cent}} \right) \Big/ \frac{\mathrm{d}^2 \sigma^{pp}_{\mathrm{jet}}}{\mathrm{d}p_{\mathrm{T}}\mathrm{d}y}$$

- ATLAS data: $\sqrt{s_{\mathrm{NN}}} = 2.76$ TeV, $\mathcal{L}_{AA} = 0.14$ nb^{-1}
  Jets identified with anti-k_{T} algorithm with $R = 0.4$
- Differential per-event jet yields in function of p_{T} in Pb+Pb collisions exhibits clear suppression with respect to pp jet cross sections (horizontal lines in the figure) for the same centrality and rapidity bins.
- The jet yields become steeper for higher rapidities.

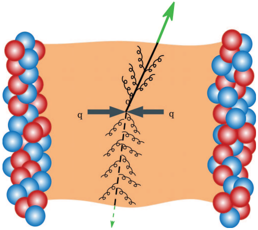

Phys. Rev. Lett. 114, 072302 (2015)

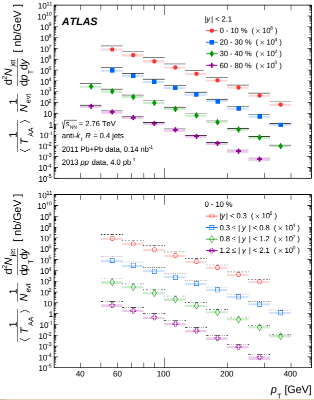

Inclusive jet suppression

- R_{AA} exhibits very slow increase with p_{T}, except in the most peripheral collisions.
- good quantitative description by theory (Y. He, I. Vitev, B.-W. Zhang, Phys. Lett. B713, 224 (2012)) - not shown.

Phys. Rev. Lett. 114, 072302 (2015)

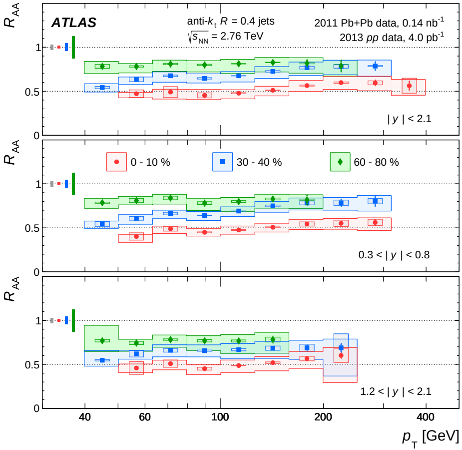

- No significant rapidity dependence, possible cancelation of two effects:
  - ↑ rapidity ⇒ steeper p_{T} spectrum ⇒ ↓ R_{AA}
  - ↑ rapidity ⇒ higher quark fraction ⇒ ↑ R_{AA}
  - Different p_{T} spectra at $\sqrt{s_{\mathrm{NN}}}$ =5 TeV may remove this cancelation.
- R_{AA} decreases smoothly from peripheral to central collisions reaching approx. 0.4 in the most central 1% of collisions.

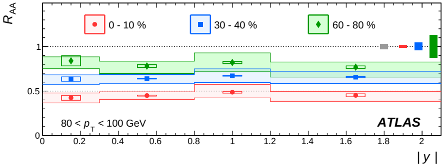

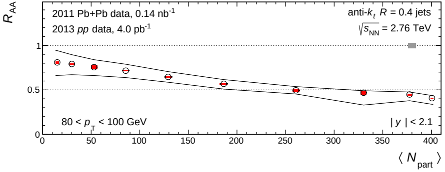

Dijet asymmetry measurement

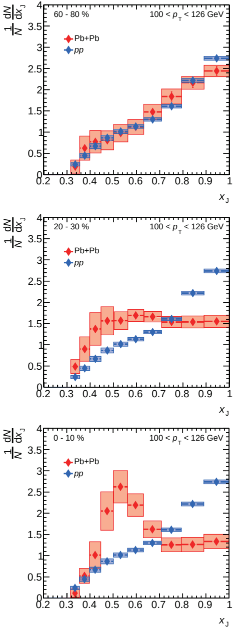

- Dijets - the jets originating from the same hard scattering can loose different amounts of energy in the medium depending on the path lengths traveled or by fluctuations.
- ATLAS data: $\sqrt{s_{NN}} = 2.76$ TeV, $\mathcal{L}_{AA} = 0.14\ \text{nb}^{-1}$
  Jets identified with anti-k_T algorithm with $R = 0.4$
  Selection of two highest p_T jets in the event with $p_T > 25$ GeV and $|\eta_{jet}| < 2.1$, which are produced back-to-back $\Delta\phi > 7\pi/8$
- Measure of dijets asymmetry used $x_J = p_{T,2}/p_{T,1},\ \ p_{T,1} > p_{T,2}$
- Increase of asymmetry with centrality of HI collisions.
- Asymmetry much less pronounced in high p_T jets sample (fluctuations of jet quenching? change of flavour composition?)

ATLAS-CONF-2015-52

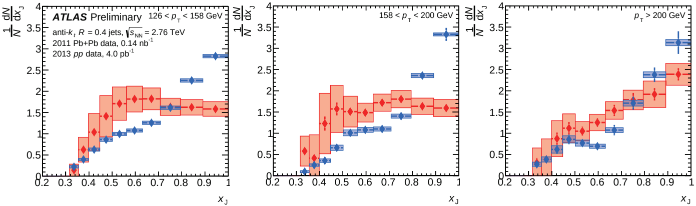

- To fully understand 'jet quenching' phenomenon, in addition to jet supression it is necessary to measure jet fragmentation i.e. possible modifications of parton showers through interactions in the plasma.

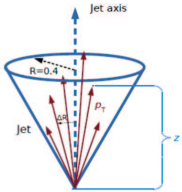

- Define jet fragmentation function as: $D(z) \equiv \frac{1}{N_{\rm jet}} \frac{{\rm d}N_{\rm ch}}{{\rm d}z}$, where $z \equiv (p_{\rm T}/p_{\rm T}^{\rm jet}) \cos \Delta R$

ATLAS-CONF-2015-55

- Distribution of charged particle transverse momenta in jet:

$$D(p_{\rm T}) \equiv \frac{1}{N_{\rm jet}} \frac{{\rm d}N_{\rm ch}}{{\rm d}p_{\rm T}}$$

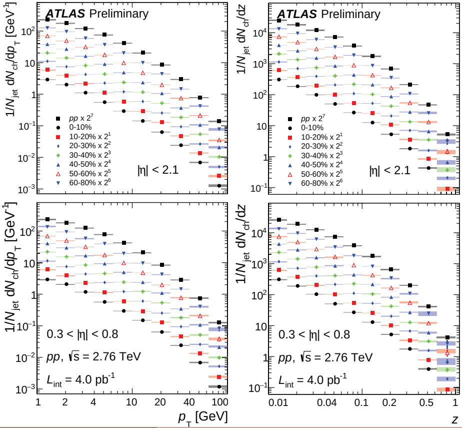

- ATLAS data: $\sqrt{s_{\rm NN}} = 2.76$ TeV
  Jet algorithm: anti-$k_{\rm T}$ with $R = 0.4$
- Measure $D(z)$ and $D(p_{\rm T})$ at the hadron level for jets in $100 < p_{\rm T}^{\rm jet} < 398$ GeV
- Difference in shape is observed between central and peripheral HI collisions or the *pp* reference.

Internal structure of jets

- To quantify this difference ratios of $D(p_{\mathrm{T}})$ and $D(z)$ measured in HI collisions to those measured in pp collisions are calculated and termed $R_{D(p_{\mathrm{T}})}$ and $R_{D(z)}$.
- Enhancement observed at low p_{T} or z and high p_{T} or z.
- Supression observed at intermediate p_{T} or z.
- This behaviour becomes less pronounced for peripheral events.
- The enhancement at high p_{T} or z becomes also less pronounced for forward jets or the jets with highest $p_{\mathrm{T}} > 158$ GeV (not shown).

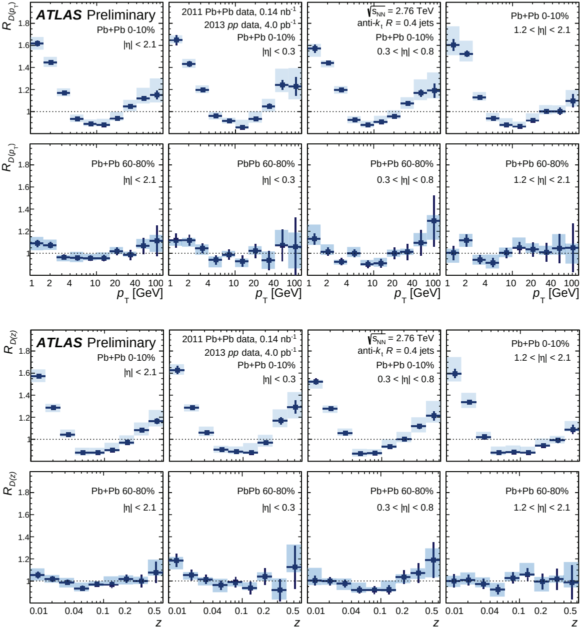

ATLAS-CONF-2015-55

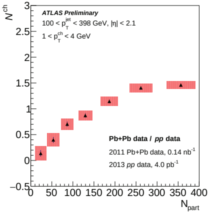

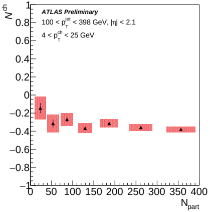

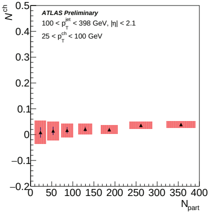

- To quantify the difference in the particle flow, the integral is used:

$$N^{\mathrm{ch}} \equiv \int_{p_{\mathrm{T,min}}}^{p_{\mathrm{T,max}}} \left(D(p_{\mathrm{T}})|_{\mathrm{cent}} - D(p_{\mathrm{T}})|_{pp} \right) \mathrm{d}p_{\mathrm{T}}$$

- Clear increase with centrality of yields of particles with low transverse momenta is observed.
  Almost no variation with centrality for intermediate and high p_{T} particle yields.
- To quantify the difference in the transverse momentum flow, the integral is used:

$$p_{\mathrm{T}}^{\mathrm{ch}} \equiv \int_{p_{\mathrm{T,min}}}^{p_{\mathrm{T,max}}} \left(D(p_{\mathrm{T}})|_{\mathrm{cent}} - D(p_{\mathrm{T}})|_{pp} \right) p_{\mathrm{T}}\, \mathrm{d}p_{\mathrm{T}}$$

- Clear increase with centrality of the transverse momentum caried by particles with low transverse momenta is observed.

ATLAS-CONF-2015-55

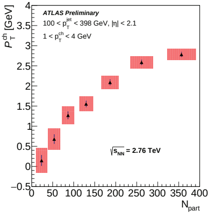

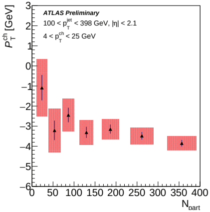

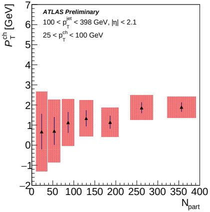

Neighbouring jets

- Studying nearby jets originating from the same hard interaction helps to disentangle between possible origins of 'jet quenching' observed in dijet events: unequal path legths of the showers in the medium or fluctuations in the energy loss process itself.

- Rate of nearby jets:
  $R_{\Delta R}(E_{\mathrm{T}}^{\mathrm{test}}, E_{\mathrm{T}}^{\mathrm{nbr}}) = \frac{1}{N_{\mathrm{jet}}^{\mathrm{test}}} \sum_{i=1}^{N_{\mathrm{jet}}^{\mathrm{test}}} N_{\mathrm{jet},i}^{\mathrm{nbr}}(E_{\mathrm{T}}^{\mathrm{test}}, E_{\mathrm{T}}^{\mathrm{nbr}}, \Delta R)$
- Calculate $\rho_{R_{\Delta R}} = R_{\Delta R}^{\mathrm{centr}} / R_{\Delta R}^{40-80\%}$
- ATLAS data: $\sqrt{s_{\mathrm{NN}}} = 2.76$ TeV
  Jets algorithm anti-k_{T} with $d = 0.4$
  Test jet: $70 < E_{\mathrm{T}}^{\mathrm{test}} < 300$ GeV;
  Nearby jet: $30 < E_{\mathrm{T}}^{\mathrm{nbr}} < 300$ GeV in annulus $0.8 < \Delta R < 1.6$ around test jet.
- Suppression becomes less pronounced with decreasing centrality.
- Decrease of suppression with increasing $E_{\mathrm{T}}^{\mathrm{nbr}}$ - comparable quenching of jets from partons of similar initial energy.

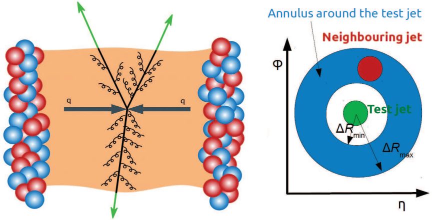

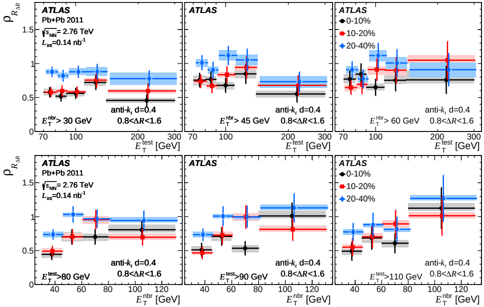

Phys. Lett. B751 (2015) 376

Bulk particle collectivity

Forward-backward multiplicity correlations

- Measurement of long range FB correlations (LRC) in full η space, with subtraction of short range correlations (SRC), performed for Pb+Pb, p+Pb and pp systems.
- Use two particle correlation function: $C(\eta_1,\eta_2) = \frac{\langle N(\eta_1)N(\eta_2)\rangle}{\langle N(\eta_1)\rangle\langle N(\eta_2)\rangle} \equiv \langle R_S(\eta_1)R_S(\eta_2)\rangle$
- But, we are interested only in dynamical fluctuations, from event to event.

So remove any residual multiplicity dependence:

$$C_N(\eta_1,\eta_2) = \frac{C(\eta_1,\eta_2)}{C_p(\eta_1)C_p(\eta_2)}$$

$$C_p(\eta_i) = \frac{1}{2Y}\int_{-Y}^{Y} C(\eta_1,\eta_2)\mathrm{d}\eta_i$$

- Estimate and subtract SRC (same source: jet fragmentation, resonant decay, ...) at $|\eta_-| \approx 0$
- Study LRC (asymmetric number of sources: strings, partons, participants, ...)
- After subtraction C_N looks similarly in all systems.

arXiv:1606.08170

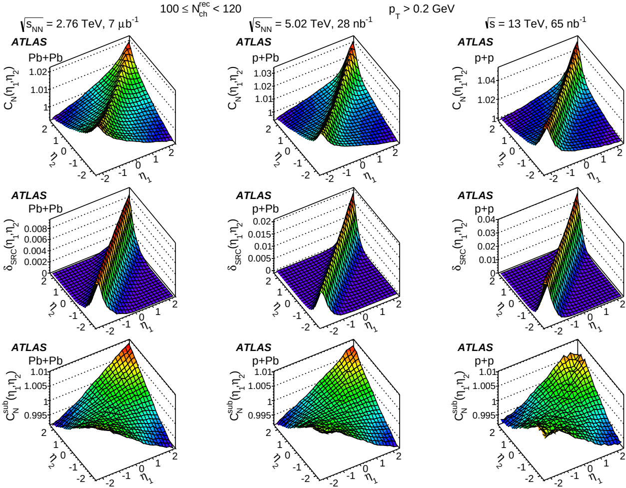

Forward-backward multiplicity correlations

- Decompose correlation function into orthogonal polynomials:

$$C_N(\eta_1,\eta_2) = 1 + \sum_{n,m=1}^{\infty} a_{n,m} \frac{T_m(\eta_1)T_m(\eta_2)+T_n(\eta_2)T_m(\eta_1)}{2}, \quad T_n(\eta) \equiv \sqrt{\frac{2n+1}{3}}\, Y\, P_n\left(\frac{\eta}{Y}\right)$$

- The two-particle Legendre coefficients are calculated from the measured $C_N(\eta_1,\eta_2)$:

$$a_{n,m} = \left(\frac{3}{2Y^3}\right)^2 \int_{-Y}^{Y} C_N(\eta_1,\eta_2) \frac{T_m(\eta_1)T_m(\eta_2)+T_n(\eta_2)T_m(\eta_1)}{2}\, d\eta_1 d\eta_2$$

- LRC are dominated by coefficient a_1 (higher order coefficients consistent with 0).
- Interpretation: LRC are dominated by linear multiplicity fluctuation in η.
- Strength of SRC defined as:

$$\sqrt{\Delta_{\mathrm{SRC}}} \equiv \frac{1}{2Y}\sqrt{\iint \delta_{\mathrm{SRC}}(\eta_1,\eta_2) d\eta_1 d\eta_2}$$

- Strength of SRC increases towards peripheral collisions (small N_{ch}).
- SRC becomes stronger in smaller systems.

arXiv:1606.08170

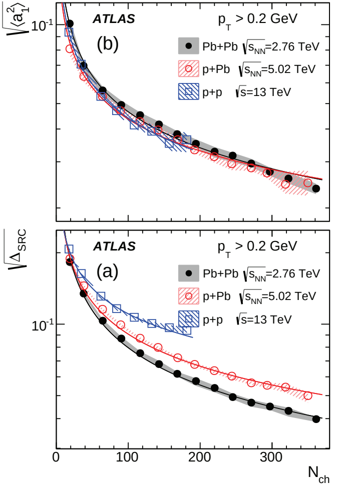

Correlations between v_2 and higher order flow harmonics

Final state momentum anisotropy is studied via Fourier decomposition of the azimuthal angle:

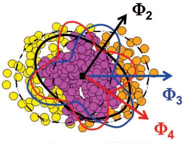

$$E\frac{d^3N}{dp^3} = \frac{1}{p_T}\frac{d^3N}{d\phi\, dp_T\, dy} = \frac{1}{2\pi p_T}\frac{E}{p}\frac{d^2N}{dp_T\, d\eta}\left(1 + 2\sum_{n=1}^{\infty} v_n \cos n(\phi - \Phi_n)\right)$$

Φ_n - azimuthal angle of the n-th order symmetry plane of the initial geometry,
$v_n \equiv \langle e^{in(\phi-\Phi_n)} \rangle = \langle \cos n(\phi - \Phi_n) \rangle$ - magnitude of the n-th flow harmonics.

- Study correlations between v_2 and v_n $(n = 2, 3, 4, 5)$ for various centrality intervals using two-particle correlation function with $|\Delta\eta| > 2$.

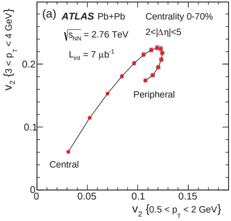

- boomerang-like structure seen in all correlation plots:
  - reflects the characteristic centrality dependence of v_2
  - is consistent with hydrodynamic predictions of stronger viscous-damping effects for v_3 than v_2 for $p_T < 3$ GeV or for $0 - 50\%$ centrality interval,
  - significant non-linear contributions to v_4 from v_2 make the boomerang-like structure less pronounced in $v_2 - v_4$ correlations.

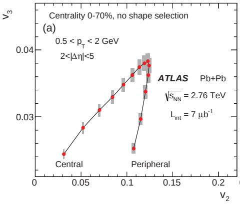

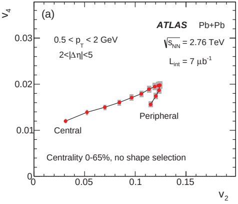

Phys. Rev. C 92, 034903 (2015)

Correlations between v_2 and higher order flow harmonics

- Events within each centrality are subdivided into q_2 (flow vector) intervals:

Phys. Rev. C 92, 034903 (2015)

$$\vec{q}_2 = \frac{1}{\sum w_i}\left(\sum[w_i \cos 2\phi_i], \sum[w_i \sin 2\phi_i]\right) - \langle\vec{q}_2\rangle_{\rm evt}$$

where $w_i = E_{\mathrm{T},i}^{\mathrm{FCal}}$

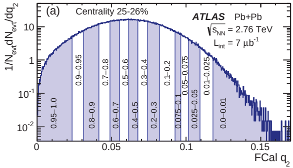

- Fix centrality (system size) and vary event shape ($\vec{q}_2$):

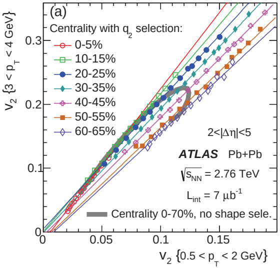

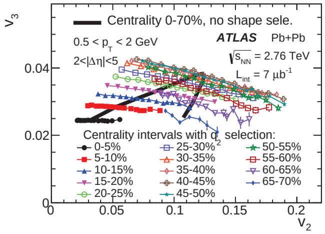

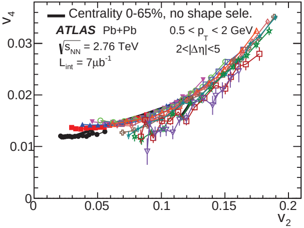

Linear correlation within given centrality $\Rightarrow$ viscous damping controlled by system size, not shape.

Clear anti-correlation, mostly initial geometry effect (AMPT calculations).

Quadratic rise from non-linear coupling to v_2^2, initial geometry does not work.

Flow non-linearity in v_4 and v_5

- v_4–v_2 correlation for fixed centrality bin: $v_4 e^{i4\Phi_4} = c_0 e^{i\Phi_4^\star} + c_1 \left(v_2 e^{i2\Phi_2}\right)^2$

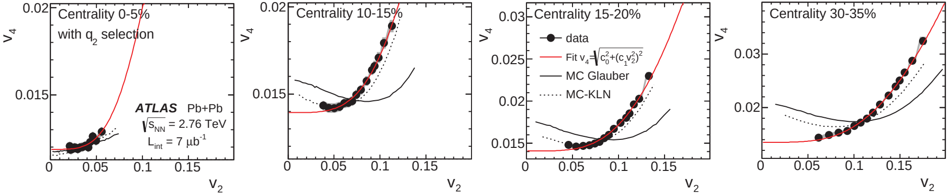

- Fit to $v_4 = \sqrt{c_0^2 + c_1^2 v_2^4}$ to separate linear and non-linear component:

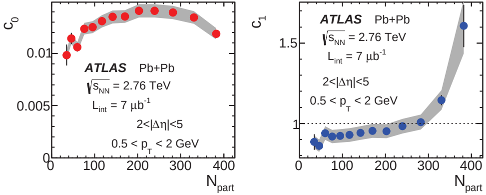

Phys. Rev. C 92, 034903 (2015)

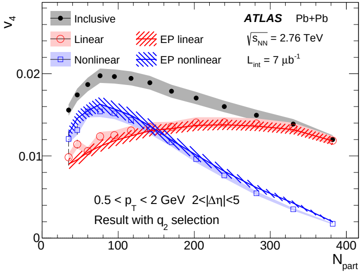

- Extract linear and non-linear terms
  $v_4^{L} = c_0, \quad v_4^{NL} = \sqrt{v_4^2 - c_0^2}$
  as a function of centrality.

- Non-linear behaviour observed also in v_5–v_2 correlation, fit $v_5 = \sqrt{c_0^2 + (c_1 v_2 v_3)^2}$.

Ultra-peripheral Pb+Pb collisions

Ultra-peripheral Pb+Pb collisions

- Ultra-peripheral collisions (UPC): $\boldsymbol{b > 2R}$
  - hadronic interactions strongly suppressed,
  - intense source of photons ($\sim Z^2$), well described by Weizsäcker-Williams (EPA).
  - maximum energy of coherent photons (Run 2):
    $E = \gamma\hbar c/R = \big\{ \gamma \approx 2805 \big\} \approx 75$ GeV

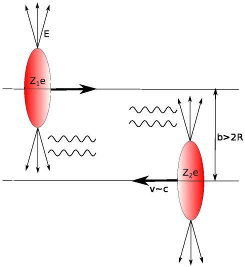

- Dileptons from photon-photon collisions:

formalism from Baltz et al. (PRC80 044902, 2009)

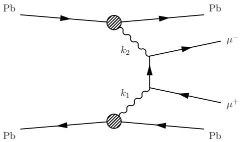

$$\frac{\mathrm{d}^2\sigma}{\mathrm{d}M_{\mu\mu}\mathrm{d}Y_{\mu\mu}} = \frac{\mathrm{d}^2\mathcal{L}_{\gamma\gamma}}{\mathrm{d}M\,\mathrm{d}Y} \times \sigma(\gamma\gamma \to \mu\mu)$$

$$\frac{\mathrm{d}^2\mathcal{L}_{\gamma\gamma}}{\mathrm{d}M\,\mathrm{d}Y} = \mathcal{L}_{AA}\frac{M}{2}\iint\limits_{b_1,b_2>R} \mathrm{d}^2b_1\mathrm{d}^2b_2\, n(k_1,b_1)n(k_2,b_2)P(b)[1-P_H(b)], \qquad b = |\vec{b}_1 - \vec{b}_2|$$

Nuclear photon flux: $n(k,b) = \dfrac{\mathrm{d}^3N}{\mathrm{d}k\,\mathrm{d}^2b} = \dfrac{Z^2\alpha}{\pi^2 k b^2}x^2K_1^2(x), \quad x = bk/\gamma$

$$\sigma_{\gamma\gamma} = \frac{4\pi\alpha^2}{W^2}\left[\left(2 + \frac{8M^2}{W^2} - \frac{16M^4}{W^4}\right)\ln\frac{W+\sqrt{W^2-4M^2}}{2M} - \sqrt{1-\frac{4M^2}{W^2}}\left(1+\frac{4M^2}{W^2}\right)\right]$$

Measurement of muon pairs in two-photon collisions

ATLAS data: Pb+Pb collisions at $\sqrt{s_{\mathrm{NN}}}$ =5.02 TeV, $\mathcal{L} = 515\ \mu\mathrm{b}^{-1}$, ZDC not used

MC simulation: STARLIGHT 1.1 (integrated over nuclear excitation states)

Signal requirements: two good muons from the common vertex with unlike signs in the fiducial range: $\boldsymbol{p_{\mathrm{T},1}, p_{\mathrm{T},2} > 4}$ **GeV**, $\boldsymbol{|\eta_1|, |\eta_2| < 2.4}$, $\boldsymbol{M_{\mu\mu} > 10}$ **GeV**

- Due to nuclear form factor, UPC dimuon pair should have $p_{\mathrm{T}} < 200$ MeV and thus small acoplanarity $(\mathrm{Aco} = 1 - |\Delta\phi|/\pi)$.
- Aco distributions show good agreement with STARLIGHT in the bulk.
- STARLIGHT does not include QED FSR, which at $\mathcal{O}(\alpha^3)$ involve and additional real photon in the final state which is expected to broaden acoplanarity distribution.
- Assuming the events with $\mathrm{Aco} > 0.008$ are primarily background, the data are fitted with two exponentials (signal [S] and bkgr. [B]): $\mathrm{d}N/\mathrm{dAco} = \sum_{i=S,B} A_i \exp\left(-\mathrm{Aco}/\alpha_i\right)$

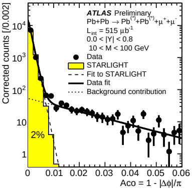

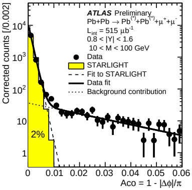

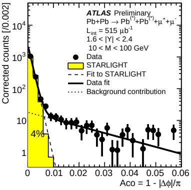

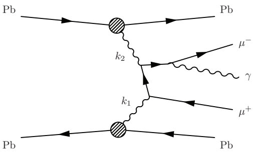

Dimuon pair cross section vs. mass and rapidity

- Both scenarios concerning the acoplanarity tails have been considered to be true:
  - the tails are all signals,
  - the tails are all backgrounds: the fits were used to extrapolate them into the signal region ($\mathrm{Aco} < 0.008$) and subtract ($2 - 4\%$ correction depending on $Y_{\mu\mu}$)

  The average of the results is presented as the central value, and half of the difference is included into systematic uncertainty.

ATLAS-CONF-2016-025

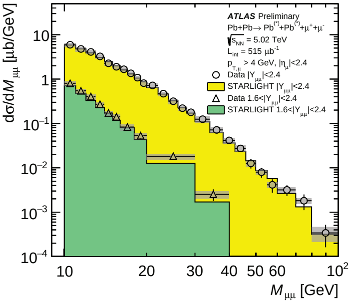

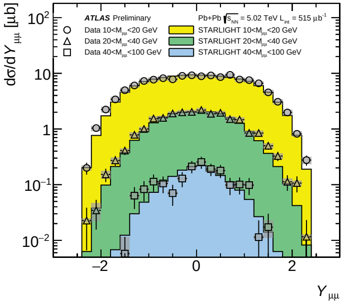

Measured differential cross sections:

- $\mathrm{d}\sigma/\mathrm{d}M_{\mu\mu}$ shown for $|Y_{\mu\mu}| < 2.4$ and $|Y_{\mu\mu}| > 1.6$
- $\mathrm{d}\sigma/\mathrm{d}Y_{\mu\mu}$ shown for $10 < M_{\mu\mu} < 20$ GeV, $20 < M_{\mu\mu} < 40$ GeV and $40 < M_{\mu\mu} < 100$ GeV
- Very good agreement with STARLIGHT truth ($\gamma = 2705$) predictions.
- Verifies both overall Z^4 scaling of $\gamma\gamma$ luminosity and γ spectrum.

Summary

ATLAS has provided several new results on all aspects of heavy ion physics:

- Probing QGP with electroweak bosons or heavy quarks does not reveal a necesity of any nuclear modifications to PDF.
- Understanding of the phenomenon of 'jet quenching' is broaden thanks to detailed study of jet production in various configurations.
- Correlations between elliptic flow in different p_{T} ranges show non-trivial centrality dependence, while they are found to be linear within narrow centrality intervals, which indicates that viscous effects are controlled by the system size, not its shape.
- Long range correlations in multiplicity are very similar in pp, p+Pb and Pb+Pb collisions.
- First measurement of two-photon production of muon pairs in lead-lead ultra-peripheral collisions has been performed.

More details and results from the heavy ion physics program realized by ATLAS is available on https://twiki.cern.ch/twiki/bin/view/AtlasPublic/HeavyIonsPublicResults

Thank you for your attention!

Backup slides

- ATLAS data: Pb+Pb at $\sqrt{s_{\rm NN}} = 2.76$ TeV, $\mathcal{L} = 0.15$ nb^{-1}, tracks with $p_{\rm T} > 0.5$ GeV
- Charged hadron yields in peripheral Pb+Pb collisions show, a $p_{\rm T}$ dependence similar to pp collisions.
- Going from peripheral to central collisions, the Pb+Pb yields increasingly deviate from pp spectra (especially for $p_{\rm T} < 1$ GeV and $10 < p_{\rm T} < 30$ GeV). This deviation is almost independent on the pseudorapidity range.
- Nuclear modification factor $R_{\rm CP}(p_{\rm T}, \eta) = \frac{\langle T_{\rm AA,P}\rangle}{\langle T_{\rm AA,C}\rangle} \frac{1/N_{\rm evt,C}\, {\rm d}^2N_{\rm Pb+Pb,C}/{\rm d}\eta {\rm d}p_{\rm T}}{1/N_{\rm evt,P}\, {\rm d}^2N_{\rm Pb+Pb,P}/{\rm d}\eta {\rm d}p_{\rm T}}$

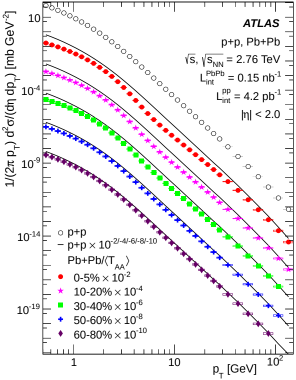

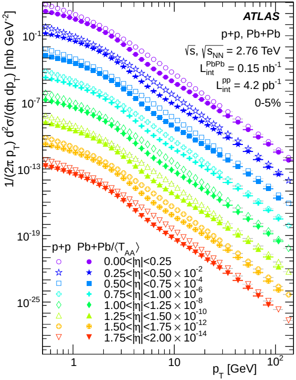

- $R_{\rm CP}$ calculated with respect to the $60-80\%$ centrality class reaches a minimum around $p_{\rm T} \approx 7$ GeV.

JHEP09 (2015) 050

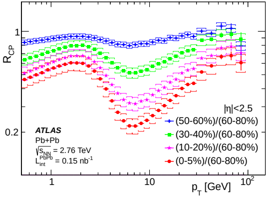

Charged-particle spectra in Pb+Pb collisions

- Nuclear modification factor $R_{\mathrm{AA}} = \frac{1}{\langle T_{\mathrm{AA}} \rangle} \frac{1/N_{\mathrm{evt}}\, \mathrm{d}^2 N_{\mathrm{Pb+Pb}}/\mathrm{d}\eta \mathrm{d}p_{\mathrm{T}}}{\mathrm{d}^2 \sigma_{pp}/\mathrm{d}\eta \mathrm{d}p_{\mathrm{T}}}$
- R_{AA} constructed from the plots from previous slide, are shown in several centrality intervals and, for most central events, in several $|\eta|$ ranges.
- R_{AA} shows a characteristic non-flat p_{T} shape: increase with p_{T} reaching maximum at $p_{\mathrm{T}} \approx 2$ GeV, then decreases reaching minimum at $p_{\mathrm{T}} \approx 7$ GeV, then again increase up to $p_{\mathrm{T}} \approx 60$ GeV and then reaches a plateau.

JHEP09 (2015) 050

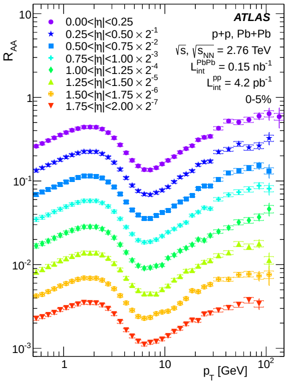

- R_{AA} has been studied as a function of $\langle N_{\mathrm{part}} \rangle$ in characteristic ranges of the p_{T} spectra.
- In all p_{T} intervals R_{AA} decreases with $\langle N_{\mathrm{part}} \rangle$, with slope being strongest for the minimum p_{T} interval and weakest for the plateau region.

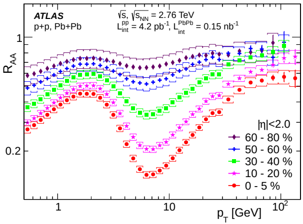

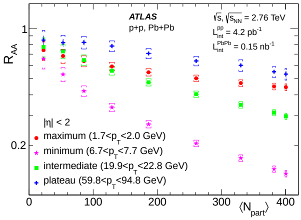

Charged-particle production in p+Pb collisions

- ATLAS data: p+Pb at $\sqrt{s_{\rm NN}} = 5.02$ TeV, $\mathcal{L} = 1\ \mu{\rm b}^{-1}$, tracks with $p_{\rm T} > 0.1$ GeV
- Differential invariant yields of charged particles produced in p+Pb collisions are measured as a function of charged particle $p_{\rm T}$ in severeal $y^\star$ intervals and as a function of $y^\star$ in several centrality intervals.

arXiv:1605.06436

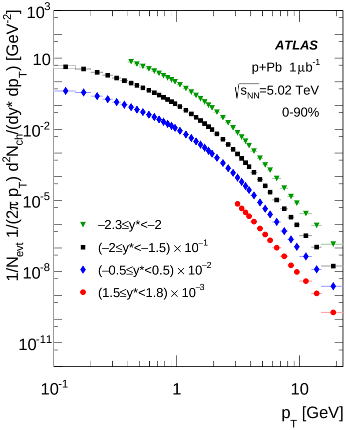

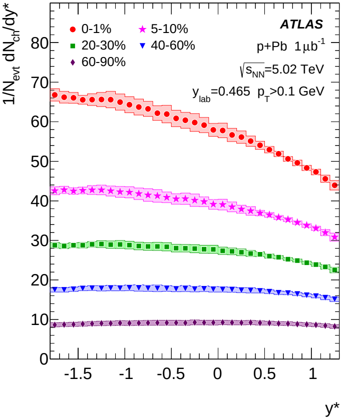

The more central collision the charged particle yields become progressively more asymmetric, with more particles produced in the Pb-going direction.

- R_{pPb} and R_{CP} distributions in different centrality intervals and for different geometrics models used to calculate $\langle T_{\mathrm{Pb}} \rangle$.
- Both R_{pPb} and R_{CP} increase with p_{T} reaching maximum at $p_{\mathrm{T}} \approx 3$ GeV and then derease with flattening above $p_{\mathrm{T}} \approx 8$ GeV.

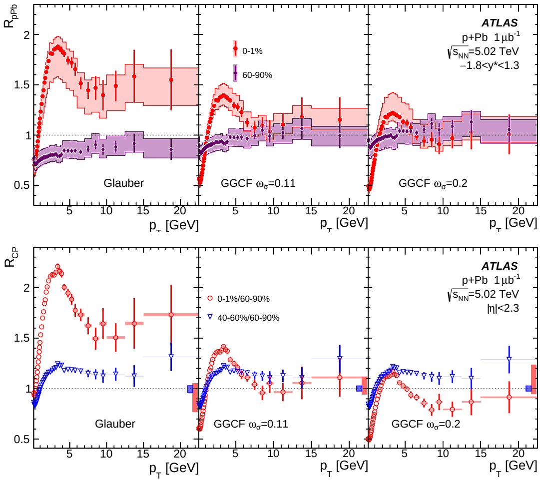

The magnitude of the peak depends significantly on the geometrical model being larger for the Glauber model than for either Glauber-Gribov models.

arXiv:1605.06436

Charged-particle spectra in p+Pb collisions

- p+Pb collisions provide insight into the effect of an extended nuclear target on the dynamics of soft and hard scattering processes and subsequent particle production.
- ATLAS data: p+Pb at $\sqrt{s_{\mathrm{NN}}} = 5.02$ TeV, $\mathcal{L} = 1\ \mu\mathrm{b}^{-1}$ Only pixel detector is used to reconstruct tracks with $p_{\mathrm{T}} > 0.1$ GeV; extrapolation to p_{T}=0 using HIJING.
- $\mathrm{d}N_{\mathrm{ch}}/\mathrm{d}\eta$ distribution has been measured as a function of pseudorapidity in several centrality intervals.
- In most peripheral collisions (60-90%) a doubly-peaked shape, similar to pp collisions, is observed.
- In more central collisions shape of $\mathrm{d}N_{\mathrm{ch}}/\mathrm{d}\eta$ bocomes progressively more asymmetric (more particles produced in Pb-going direction).
- If the $\mathrm{d}N_{\mathrm{ch}}/\mathrm{d}\eta$ distribution in each centrality interval is scaled by the distribution for most peripheral collisions, then the double-peak structure disappears.
- The ratios grow nearly linearly with decreasing pseudorapidity, with a slope whose magnitude increases towards more central collisions.

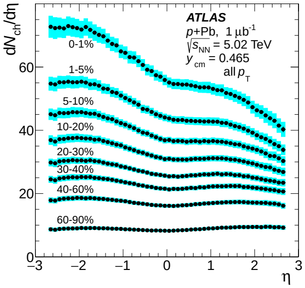

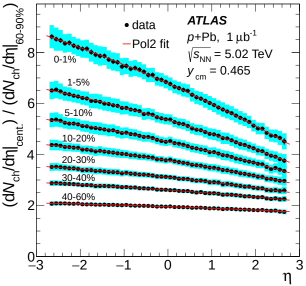

Eur. Phys. J. C (2016) 76:199

Charged-particle spectra in p+Pb collisions

- Distributions of $\mathrm{d}N_{\mathrm{ch}}/\mathrm{d}\eta$ per participant pair, $\langle N_{\mathrm{part}}\rangle/2$, for the most central and most peripheral events as a function of η for different models of collisions geometry.
- Results for most peripheral events are almost model independent.
  More particles produced in the proton-going direction due to higher energy of the proton compared to the energy of a single nucleon in the lead nucleus in LAB.
- In most central interval more particles are produced in the Pb-going direction and the magnidude of the distributions strongly depends on the geometric model.

- When ploted vs. $\langle N_{\mathrm{part}}\rangle$ the distributions are almost constant up to $\langle N_{\mathrm{part}}\rangle \approx 10$, but above this value start to depend on the model.

Eur. Phys. J. C (2016) 76:199

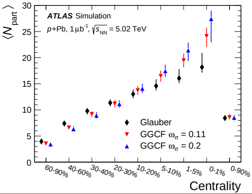

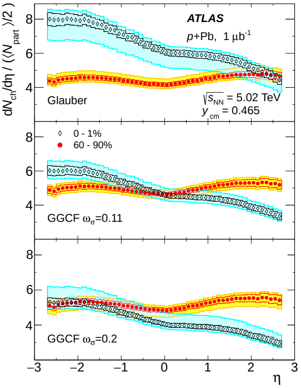

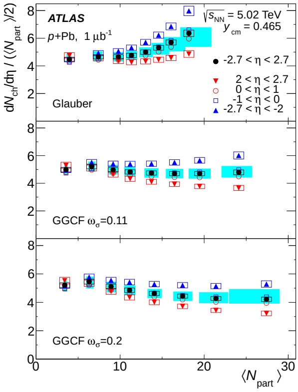

Dimuon production in UPC

- Distributions of single muons after full dimuon selection and correction for trigger efficiency show very good agreement with STARLIGHT predictions.
- Systematic uncertainties:
  - Muon trigger efficiency:
    MB and T&P methods agree up to 5%
  - Muon reconstruction efficiency:
    differences between data and simulation $2-5\%$
  - Background subtraction:
    uncertainty related to acoplanarity tail $6-10\%$
  - Vertex efficiency: data vs. MC difference 2%
  - MC closure is good up to 2% level
  - Luminosity uncertainty assigned to be 7%

Overall systematic uncertainty $10-12\%$.

ATLAS-CONF-2016-025